



A Markov chain Monte Carlo algorithm for upscaled soil-vegetation-atmosphere-transfer modeling to evaluate satellite-based soil moisture measurements

N. N. Das,¹ B. P. Mohanty,¹ and E. G. Njoku²

Received 27 August 2007; revised 29 January 2008; accepted 25 February 2008; published 20 May 2008.

[1] A Markov chain Monte Carlo (MCMC) based algorithm was developed to derive upscaled land surface parameters for a soil-vegetation-atmosphere-transfer (SVAT) model using time series data of satellite-measured atmospheric forcings (e.g., precipitation), and land surface states (e.g., soil moisture and vegetation). This study focuses especially on the evaluation of soil moisture measurements of the Aqua satellite based Advanced Microwave Scanning Radiometer (AMSR-E) instrument using the new MCMC-based scaling algorithm. Soil moisture evolution was modeled at a spatial scale comparable to the AMSR-E soil moisture product, with the hypothesis that the characterization of soil microwave emissions and their variations with space and time on soil surface within the AMSR-E footprint can be represented by an ensemble of upscaled soil hydraulic parameters. We demonstrated the features of the MCMC-based parameter upscaling algorithm (from field to satellite footprint scale) within a SVAT model framework to evaluate the satellite-based brightness temperature/soil moisture measurements for different hydroclimatic regions, and identified the temporal effects of vegetation (leaf area index) and other environmental factors on AMSR-E based remotely sensed soil moisture data. The SVAT modeling applied for different hydroclimatic regions revealed the limitation of AMSR-E measurements in high-vegetation regions. The study also suggests that inclusion of soil moisture evolution from the proposed upscaled SVAT model with AMSR-E measurements in data assimilation routine will improve the quality of soil moisture assessment in a footprint scale. The technique also has the potential to derive upscaled parameters of other geophysical properties used in remote sensing of land surface states. The developed MCMC algorithm with SVAT model can be very useful for land-atmosphere interaction studies and further understanding of the physical controls responsible for soil moisture dynamics at different scales.

Citation: Das, N. N., B. P. Mohanty, and E. G. Njoku (2008), A Markov chain Monte Carlo algorithm for upscaled soil-vegetation-atmosphere-transfer modeling to evaluate satellite-based soil moisture measurements, *Water Resour. Res.*, 44, W05416, doi:10.1029/2007WR006472.

1. Motivation

[2] Studies [Claussen, 1998; Delworth and Manabe, 1989; Foley, 1994; Texier *et al.*, 1997] have shown that the initial/boundary (I/BC) values of state variables (e.g., soil moisture, soil temperature, vegetation water content) at various spatial and temporal scales in the land surface exert strong controls on hydrologic, climatic, and weather related processes. Hence measuring these state variables is crucial for flood forecasting, natural resource management, agronomic crop management, and regional/global climate simulation. There are various ways to measure the state variables depending upon the spatial scale of interest. In

situ techniques provide reasonably accurate measurements of state variables at the local scale, at desired time intervals. Direct incorporation of in situ measurements as I/BC in large-scale models has limitations due to its very small spatial support. Satellite-based remote sensors measure spatially integrated measurements of state variables with temporal sampling that depends upon the orbital placement of the satellites. This makes satellite-based measurements suitable for I/BC in large-scale modeling. However, the quality of satellite-based land parameter measurements is often questionable due to uncertainties introduced by atmospheric attenuation, clouds, rainfall, and the inherent variability present in geophysical properties and state variables, which influence the measurements and their calibration and validation. The extent and spatial resolution of satellite-based measurements can also introduce complex scale effects [Western *et al.*, 2002]. Conventionally, satellite-based measurements are validated using ground-based measurements, but this approach is also limited in accounting for scale effects and heterogeneity within the large footprints. In this study we focus primarily on developing

¹Department of Biological and Agricultural Engineering, Texas A&M University, College Station, Texas, USA.

²Water and Carbon Cycles Group, Jet Propulsion Laboratory, California Institute of Technology, Pasadena, California, USA.

a physically based soil hydrologic model at the satellite footprint scale, including parameter upscaling and a soil moisture data assimilation scheme.

[3] The Advanced Microwave Scanning Radiometer (AMSR-E) on the Earth Observing System Aqua satellite is currently used for global soil moisture mapping [Njoku *et al.*, 2003]. AMSR-E measures radiation at six frequencies in the range 6.9–89 GHz with dual polarization. It covers the globe in approximately 2 days or less with a swath of 1445 Km. The spatial resolution at the surface varies from approximately 60 Km at 6.9 GHz to 5 Km at 89 GHz [Njoku *et al.*, 2003]. The current AMSR-E soil moisture algorithm is based on a change detection approach using polarization ratios (PR) of the calibrated AMSR-E channel brightness temperatures [Njoku and Chan, 2006]. The accuracy of the soil moisture algorithm has been investigated on short timescales during calibration/validation field campaigns of the Soil Moisture Experiments in 2002, 2003, and 2004 (SMEX02, SMEX03, and SMEX04) [Bindlish *et al.*, 2006, 2008; Jackson *et al.*, 2005]. Results show some level of consistency and calibration stability of the observed brightness temperatures at specific locations. However, there have been concerns regarding the spatial variability of the retrieved soil moisture biases over areas with different amounts of vegetation. AMSR-E measurements have shallow measurement depth (1 cm or less) and coarse spatial resolution (~60 km) at 10.7 GHz, which, combined with subgrid and grid scale variability, also impose limitations on the retrieval algorithm and its operational accuracy.

[4] Measurements of microwave emissions show sensitivity to soil moisture through the effects of moisture on the dielectric constant and hence emissivity of the soil [Ulaby *et al.*, 1986]. The large contrast between the real part of the dielectric constant of water and that of dry soil translates into a difference of up to 100 K or more in brightness temperature between very dry and very wet soils [Njoku and Kong, 1977; Wang, 1980; Wang and Choudhury, 1995]. The surface geophysical properties, i.e., soil characteristics (surface roughness and soil texture) and vegetation, also affect the microwave emissivity. Vegetation acts as an attenuating and emissive layer over the soil [Jackson and Schmugge, 1991; Njoku and Chan, 2006; Ulaby and Wilson, 1985] and is characterized mainly by its water content and geometrical structure. The net effect of vegetation is a reduction in sensitivity that makes it more difficult to estimate soil moisture accurately over vegetated terrain. At AMSR-E frequencies (6.6 GHz and higher) the sensitivity to soil moisture becomes very low when the leaf area index (LAI) exceeds 2.0 [Njoku and Li, 1999]. Surface roughness adds another dimension of complexity due to surface scattering [Choudhury *et al.*, 1979; Njoku and Chan, 2006], which affects the emissivity. The net effect of surface roughness can be difficult to establish, especially when dealing with inhomogeneous elements. Soil texture, ranging from sand to clay, also influences the emissivity of the soil. Sandy soil has the highest emissivity at all frequencies, which is influenced by least specific surface area of soil that leads to lowest bound water [Wang and Schmugge, 1980].

[5] The uncertainty in estimating microwave emissivity at the AMSR-E footprint scale is affected also by the heterogeneity of the vegetation, surface roughness, and soil moisture within the footprint. Soil moisture exhibits hetero-

geneity due to variability in a number of geophysical parameters (soil properties, vegetation, topography, and precipitation). The soil moisture distribution at a particular spatiotemporal scale within an AMSR-E footprint evolves from complex interactions among these geophysical parameters [Dubayah *et al.*, 1997; Western *et al.*, 2002]. Soil properties always exhibit significant spatial variability that characterizes the soil moisture status and transport processes. For example, Rodriguez-Iturbe *et al.* [1995] suggested that the spatial organization of soil moisture is a consequence of the soil properties; Tomer *et al.* [2006] found significant correlation between soil properties and soil moisture at the watershed scale; and [daSilva *et al.*, 2001] showed that temporal stability in soil moisture patterns can be associated with the arrangement of soil types and textures at the landscape scale. Soil texture is also related to topographical attributes such as surface curvature, slope, and elevation. Mohanty and Mousli [2000], Pachepsky *et al.* [2001], and Leij *et al.* [2004] demonstrated that soil hydraulic properties relate to relative landscape positions in topographically complex landscapes, and Chang and Islam [2003] demonstrated that soil physical properties and topography together control spatial variations of soil moisture over large areas. They showed that topographical control dictates the soil moisture distribution under wet conditions, and soil physical properties control variations of soil moisture under relatively dry conditions. Infiltration properties of soil are influenced by vegetation at the plant scale [Seyfried and Wilcox, 1995] or tillage/cropping practice at the field scale [Mohanty *et al.*, 1994b]. In a recent study, Sharma *et al.* [2006] discovered that including remotely sensed vegetation parameters in addition to soil texture and topographic features improved the predictability of soil hydraulic properties across Little Washita watershed in Oklahoma using artificial neural networks. These spatially overlapping geophysical attributes define the functional organization of soil hydrological processes and, in turn, soil moisture variability. The evolution of the soil moisture state within the AMSR-E footprints is primarily forced by precipitation. For this study, subgrid variability of precipitation is not considered. The partitioning and transport of the water above and below the land surface is controlled mainly by soil hydraulic properties, which are in turn influenced by soil types, texture, topography, and vegetation. In summary, the emitted microwave radiation (brightness temperature) of the soil observed at the 60-km × 60-km AMSR-E footprint scale is a weighted integral of the soil moisture distribution, as influenced by the variability in soil hydraulic properties within the footprint. Camillo *et al.* [1986] have also shown that remotely sensed soil moisture may be inverted to estimate soil hydraulic properties using a microwave emission model and soil moisture and temperature profiles generated by moisture and energy balance equations. Application of such approaches on a regional scale may generate large-scale soil properties for input into mesoscale land-atmosphere models. Regional soil properties may be estimated by inversion of a dynamic one-dimensional soil-water-vegetation model in conjunction with soil moisture obtained from microwave remote sensing.

[6] On the basis of the above discussion we hypothesize that an ensemble of soil hydraulic properties describing the soil moisture dynamics within the AMSR-E footprint can be

used to compare with the soil moisture estimated from microwave emission of the surface soil layer. In other words, the ensemble of soil hydraulic properties can suitably characterize the variability present within the AMSR-E footprint. Although at a field scale, *Burke et al.* [1997] demonstrated retrieval of soil hydraulic properties from the time series of the measured brightness temperature over agricultural fields. There could be some concern, however, about the validity of using an ensemble of local soil hydraulic properties to represent conditions at the remote sensing footprint scale. Soil hydraulic properties are defined at the point to field scale, whereas soil is conceptualized as a hierarchical heterogeneous medium with discrete spatial scales [e.g., *Roth et al.*, 1999]. It is argued that the natural pattern of soil variability may exhibit embedded, organizational structures that lead to nonstationary soil hydraulic properties and processes. With an increase in spatial scale (support), soil hydraulic properties typically become nonstationary. The soil hydraulic properties may change from deterministic at smaller scale to more random at larger scale, with the small-scale soil properties filtered out by larger-scale soil-related processes [*Kavvas*, 1999]. Thus upscaling of soil properties is required to understand the physical processes and to characterize the evolution of soil moisture and, in turn, soil emissivity, at the AMSR-E footprint scale.

[7] The primary objective of this study is to develop a procedure, using a Markov Chain Monte Carlo (MCMC) algorithm, for estimating upscaled land surface parameters to be used in a SVAT model for evaluating satellite-based land surface state measurements. The performance of the upscaled parameters and SVAT model can then be tested using selected AMSR-E footprints in three different hydroclimatic conditions to evaluate the satellite-based soil moisture product.

2. Approach

[8] Effective soil hydraulic parameters are a representative set of parameters that characterize a footprint-scale domain and approximate the flux equivalent to the aggregated flux obtained from distributed modeling within the domain [*Kabat et al.*, 1997; *Zhu and Mohanty*, 2003]. Footprint-scale effective soil hydraulic parameters are vital to hydroclimatic studies since such studies commonly use soil-vegetation-atmosphere-transfer (SVAT) models whose subsurface flow components are based on the Darcian flow equation [*Demarty et al.*, 2005]. The soil hydraulic parameters used in SVAT models are physically defined at a local measurement scale (mostly at point to field scale). Therefore soil hydraulic parameter upscaling from field scale to hydroclimate grid or satellite footprint scale is critical for SVAT model performance at these scales. The difficulty of upscaling soil hydraulic parameters to the footprint scale stems from the inherent spatial variability of soil properties and the nonlinear dependence of soil moisture. Our strategy here is to develop a new approach for estimating upscaled soil hydraulic parameters. We follow a method that derives upscaled hydraulic parameters directly from explicit information on the soil moisture state at the AMSR-E footprint scale and the stochastic variability of soil hydraulic parameters at the much smaller (local) scale within the footprint. Using ensembles of upscaled soil hydraulic parameters, large-scale fluxes and states at the land surface can be

determined that are compatible with the microwave emission from the surface soil layer at the footprint scale.

[9] The algorithm developed for this approach uses a Bayesian methodology that provides an effective and efficient tool for combining two or more discrete sources of information, model output, and observed data. The algorithm is used to merge prior information on an arbitrary number of soil hydraulic parameters, with the information content of the related soil moisture data, to find SVAT model parameter estimates. The algorithm is particularly useful when extracting target (soil hydraulic property) characteristics from remotely sensed (e.g., AMSR-E soil moisture) data. The Bayesian technique can produce full probability distributions for an arbitrary number of parameters. In practice, the probability distributions can be considered to represent either the imprecise knowledge regarding the true value of the parameter, the natural variability of the parameter, or a combination of the both. In the procedure, the inference about the set of soil hydraulic parameters is obtained after integrating all possible combinations of the soil hydraulic parameters in the full joint probability posterior distribution. In this study the integration is performed on the set of parameters using a Markov Chain Monte Carlo (MCMC)-based numerical method.

2.1. MCMC Algorithm

[10] Bayesian methods provide a framework within which preexisting knowledge about the parameters of a model can be combined with observed data and model output. This results in a probability distribution of the parameter space (posterior distribution) that summarizes uncertainty about the parameters based on the combination of preexisting (or prior) knowledge and the sampled data values. In this study, the uncertainties in accurately determining the parameters of the nonlinear soil water retention function for large-scale hydrological modeling is the focus of the development of the Bayesian framework. The Bayesian approach takes the parameters of the model as random variables [*Gelman et al.*, 1995] with particular probability density functions (pdf's). Thus, in addition to the determination of a likelihood function, the process of Bayesian inference may require the specification of prior pdf's that summarize the prior knowledge. Figure 1 illustrates the methodology of the Bayesian framework. Here the likelihood function is the time series of AMSR-E derived soil moisture data $D = \{\theta_1, \theta_2, \dots, \theta_i\}$ at a particular grid point. The priors are defined as the soil hydraulic parameters (shown in equation (1)) of the dominant soil types based on Soil Survey Geographic (SSURGO) database within the particular AMSR-E footprint. These soil hydraulic parameters are used in the Mualem–van Genuchten functions [*Mualem*, 1976; *van Genuchten*, 1980]:

$$S_e = \frac{\theta(h) - \theta_{res}}{\theta_{sat} - \theta_{res}} = \left[\frac{1}{1 + |\alpha h|^n} \right]^m \quad (1)$$

$$K(h) = K_{sat} S_e^\lambda \left[1 - \left(1 - S_e^{1/m} \right)^m \right]^2, \quad (2)$$

where water content θ is a nonlinear function of pressure head h , S_e is the relative saturation ($\theta - \theta_{res} / \theta_{sat} - \theta_{res}$), θ_{res} and θ_{sat} are the

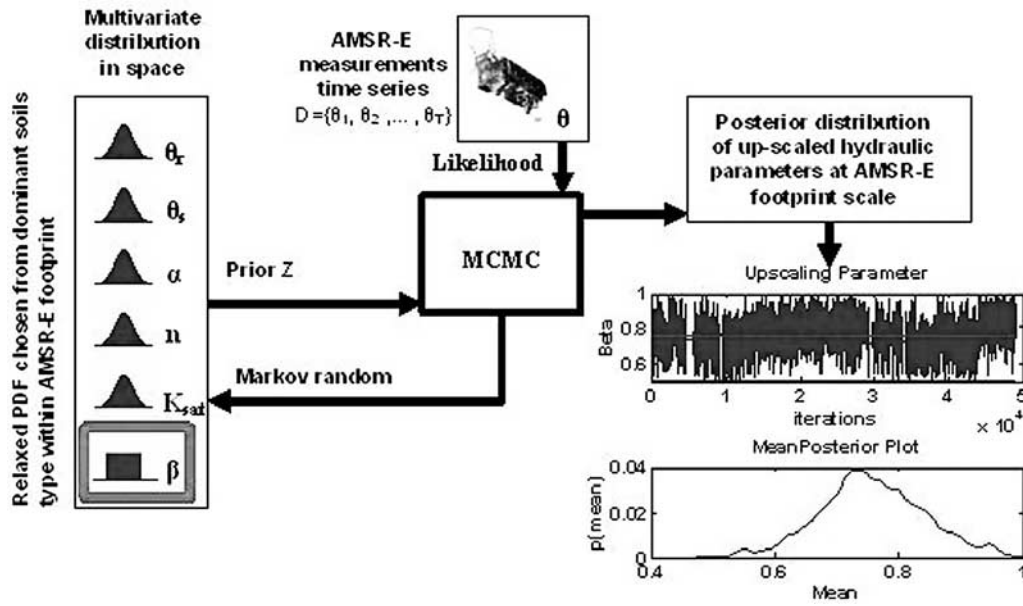


Figure 1. Markov chain Monte Carlo (MCMC) based schematic for deriving upscaled soil hydraulic parameters.

residual and saturated water contents ($\text{cm}^3 \text{cm}^{-3}$) respectively, α (cm^{-1}), n (cm^{-1}), m (cm^{-1}), and λ (cm^{-1}) are shape parameters of the retention and the conductivity functions, K_{sat} is the saturated hydraulic conductivity (cm d^{-1}), and $m = 1 - 1/n$. The values of these parameters are distinct among soil (textural) types and are defined at the local or field scale. By virtue of the variability in soil types within an AMSR-E footprint, very relaxed pdf's (high standard deviations, σ) were defined for the soil parameters as priors. A normal distribution was assigned to all parameters, e.g., $\theta_{res} \sim N(\mu_{\theta_{res}}, \sigma_{\theta_{res}})$ based on the UNSODA database [Nemes *et al.*, 2001]. In principle, nonnormal priors could be used as well, but the computational complexity would increase considerably. If no prior information from the SSURGO database is available for the soil parameters except for their ranges, uniform pdf's are assigned in the valid ranges. For computational simplicity, random samples are drawn independently from the pdf's of different soil hydraulic parameters to form a field-scale parameter set $(\theta_r, \theta_s, \alpha, n, K_{sat})$. A scaling parameter β is introduced in our algorithm to account for the scale disparity. The scaling parameter β has a noninformative prior distribution (i.e., uniform distribution) that gives no preference to any parameter definition domain. However, it can be noted that a noninformative prior gives information on the parameter limit values i.e., a uniform distribution between 0 and 1. Thus β relates the soil hydraulic parameters at the field scale to the effective soil hydraulic parameters at the AMSR-E footprint scale. The general relationship used in this study for upscaling of any of the soil hydraulic parameters in the Mualem–van Genuchten relationship (equation (1)) can be written as (e.g., for θ_r)

$$(\theta_r)_{\text{eff}} = (\theta_r)^\beta, \quad (3)$$

where $(\theta_r)_{\text{eff}}$ is the effective value of the residual water content at the AMSR-E footprint scale. For flat homogenous

bare soil the value of β is 1 and the parameter values are independent of spatial scale. With heterogeneity the value of β remains no longer equal to unity and in fact can be larger or smaller than one. The study found the upscaling factor β smaller than 1 due to heterogeneity introduced by soil types, vegetation, and atmospheric forcings with increasing spatial scale. Essentially, all the nonlinearity encountered in the physical processes with increasing spatial scale is lumped in the scaling factor β . Thus, for upscaling the field-scale parameters, equation (3) was used to form a set of upscaled parameters, $z_i = (\theta_{res}^{\beta_i}, \theta_{sat}^{\beta_i}, \alpha^{\beta_i}, n^{\beta_i}, K_{sat}^{\beta_i})$, where i is a realization of the MCMC and the upscaling parameter β_i represents the corresponding upscaling parameter drawn randomly from a uniform distribution between 0 and 1.

[11] By applying Bayes' theorem, the conditional posterior pdf, $P(Z|D)$, given the measured values of D (vector of AMSR-E soil moisture data), is described as

$$P(Z|D) = \frac{P(Z)P(D|Z)}{P(D)}, \quad (4)$$

where $P(Z)$ is the prior joint pdf for the upscaled soil hydraulic parameters $Z = \{z_1, z_2, \dots, z_m\}$. The $P(D)$ is a normalization factor, and $P(D|Z)$ is the likelihood derived from measured AMSR-E soil moisture footprint values given Z . To describe the AMSR-E data, a normal (pdf) likelihood was introduced. Once the joint pdf is obtained, given specific values for D , the marginal posterior can be obtained back to beginning PDF that retains exclusively the dependence on one parameter (e.g., θ_{res}^β) can be obtained as follows:

$$P(\theta_{res}^\beta|D) = \frac{\int \int \int \int P(D|Z)P(Z)d\theta_{sat}^\beta d\alpha^\beta dn^\beta dK_{sat}^\beta}{P(D)} \quad (5)$$

$$P(D|Z) \propto \prod \frac{\exp\left(\frac{(D-\theta(h))^2}{2\sigma^2}\right)}{\sigma} \quad (6)$$

$$P(Z) \propto \exp\left(-\frac{1}{2}(Z-\mu)^T \Sigma^{-1}(Z-\mu)\right), \quad (7)$$

where Σ is the covariance matrix of the soil hydraulic parameters, σ is the standard deviation of D , and μ is the vector of means of the parameters. This marginalization could potentially be an intractable task because of the high-dimensional integration in equation (5). This could happen when the retrieval process is applied to situations where there are more than two soil parameters to be estimated, and when the resulting PDF does not have a standard form. A possible solution is to estimate the form of the posterior PDF by generating samples by means of the Markov Chain Monte Carlo (MCMC) method [Brooks and Roberts, 1998]. The mean, variance, and higher-order moments for the parameters can be calculated from the numerically approximated PDFs of the MCMC. We use the MCMC to perform the integration required for the evaluation of equation (5). More specifically, we used the Metropolis algorithm for the Markov Chain Monte Carlo (MCMC) method with a simple random walk to describe the posterior distribution, representing the ensemble of soil hydraulic parameters for the AMSR-E footprint. The Metropolis algorithm [Metropolis and Ulam, 1949] has been widely used in Bayesian applications because of its simplicity and its efficiency. Its principle can be summarized as follows: Starting from a vector generated at iteration $i - 1$, a new candidate vector is generated based on a symmetric jump distribution. The symmetric jump distribution depends on candidate vector generated at iteration $i - 1$ and explores the surroundings of candidate vector. The SVAT model (addressed below) is run with the new candidate vector (proposed soil hydraulic parameters), and the surface soil moisture generated from the model is compared with the AMSR-E measurements. If this new candidate vector leads to an increased probability of the target (i.e., posterior) distribution, it is accepted as the generated value at iteration i . Otherwise, the ratio between the new and the previous value of the target distribution is computed, and used as the acceptance probability of the candidate vector. In case of rejection, the generated vector at iteration i remains the same as that at iteration $i - 1$. The Metropolis algorithm was used in this paper with a Gaussian jump distribution with covariance matrix Σ . The MCMC algorithm used in the study is summarized below:

[12] 1. Choose a starting point of candidate vector $\pi(0)$ with a covariance matrix Σ .

[13] 2. Iterate $i = 1, \dots, N_{iter}$

[14] 3. Generate a candidate vector based on $\pi^* \sim N(\pi^{(i-1)}, \Sigma)$.

[15] 4. If $p(\pi^*|X) \geq p(\pi^{(i-1)}|X)$, set $\pi(i) = \pi^*$, else accept the candidate vector ($\pi(i) = \pi^*$) with probability $r = \frac{p(\pi^*|X)}{p(\pi^{(i-1)}|X)}$ or reject it ($\pi(i) = \pi^{(i-1)}$) with probability $(1 - r)$.

[16] In order to avoid numerical overflows, it is useful to consider the logarithm of the posterior distribution, and to compute the posterior ratio as $r = \exp(\log(p(\pi^*|X)) - \log(p(\pi^{(i-1)}|X)))$. Moreover, this ratio is made invariant by multiplying the posterior distribution by a constant, which

implies that the Metropolis algorithm can be applied to a nonnormalized target distribution. The MCMC algorithm generates a Markov chain (k_n) whose stationary distribution is $\pi(k)$. The posterior distributions of parameters obtained from the MCMC algorithm are further subjected to a process of thinning. The objective of thinning is to decrease the autocorrelation (increasing independence) between samples. Thinning a Markov chain necessitates that the chain be long enough to obtain a sample of the desired size. Thinning was implemented in the algorithm by periodic selection of samples from the MCMC chain at a specified rate to form an ensemble of soil hydraulic parameters.

2.2. SVAT Modeling for Soil Moisture Estimation

[17] Key challenges in using SVAT models for very coarse scale (e.g., AMSR-E footprint scale) hydrologic modeling are the selection of governing flow equations, setting accurate boundary conditions, and defining the modeling domain. For this study, we used the parallel noninteracting soil column approach [Milly, 1988; Peck et al., 1977] that allows a variety of modeling concepts for soil water processes in heterogeneous conditions. In this stream-tube approach, the horizontal spatial heterogeneity is represented by an ensemble of upscaled soil hydraulic parameters and is conceptualized as bundle of independent parallel soil columns. At the large spatial scale, the stream tube approach suits well the hypothesis of negligible lateral interflow across adjacent soil columns within the modeling domain. In a previous study, Zhu and Mohanty [2002] analyzed the magnitude of the lateral flow component in parallel soil columns and found them of minor importance. We also assumed that the 1-D Richards' equation is an appropriate physical model to simulate the vertical partially saturated flow and partitioning of fluxes at such coarse spatial scale. Numerical studies conducted by Mantoglou [1992] and Zhang [1999] on general upscaled Richards' equations have shown that at large spatial scales and in the absence of lateral flow, vadose zone flow can be represented by the one-dimensional Richards' equation. We used the SWAP model [Van Dam et al., 1997] to simulate the processes of the soil-water-atmosphere-plant system. SWAP is a physically based, hydrologic model that numerically solves the one-dimensional Richards' equation for simulating the soil moisture dynamics in the soil profile under different climatic and environmental conditions. Irrespective of scale, for transient isothermal unsaturated water flow in nonswelling soil, Richards' equation as used in SWAP is described by

$$\frac{\partial \theta}{\partial t} = \frac{\partial}{\partial z} \left[K \left(\frac{\partial h}{\partial z} + 1 \right) \right] - S_a(h), \quad (8)$$

where θ is the soil water content (m^3/m^3), z is the soil depth (m), h is the soil water pressure head (m), K is the unsaturated hydraulic conductivity (m/d), and $S_a(h)$ is the sink term i.e., root water uptake (m/d). The Penman-Monteith equation [Monteith, 1965] was used to calculate potential evapotranspiration, while potential transpiration (T_p) and soil evaporation (E_p) were partitioned using LAI. In the SWAP model, soil moisture retention and hydraulic conductivity functions are defined by the Mualem-van Genuchten equations, shown in equations (1) and (2), respectively.

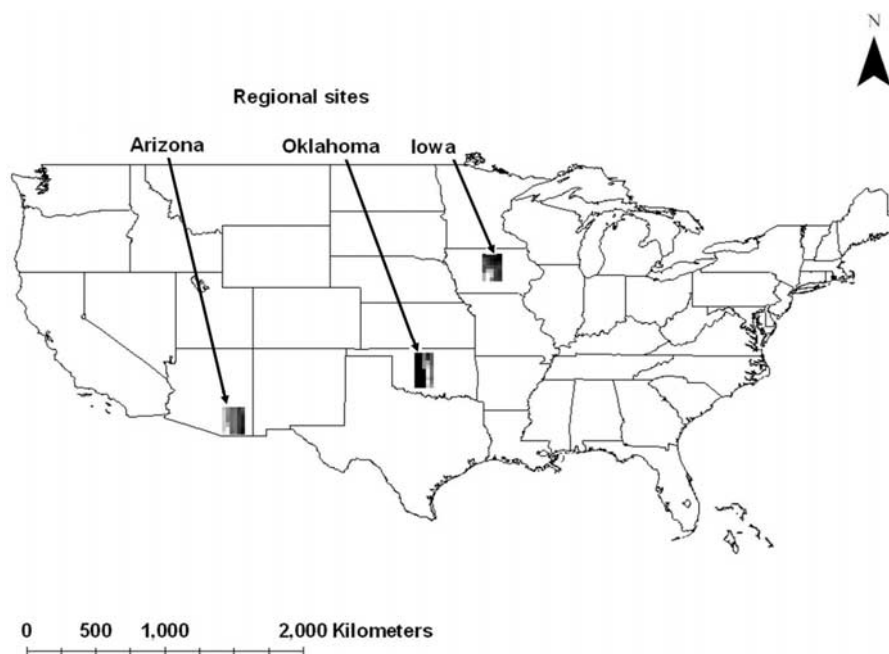


Figure 2. Three selected study regions (Arizona, Oklahoma, and Iowa) within the continental United States of America.

[18] SWAP is a numerical water management tool that can accommodate several combinations of top and bottom boundary conditions. Availability of satellite data to characterize the upper boundary condition as well as the vegetation cover allows study of regional/footprint scale soil water processes. The SWAP model simulates both the soil water quantity and quality with a temporal resolution of 1 day, along with other state variables. The model has been used in various applications in the past and has been well validated under different climatic and environmental conditions [Ines and Droogers, 2002; Ines and Mohanty, 2008; Wesseling and Kroes, 1998]. For more detailed descriptions of SWAP the reader can refer to Van Dam [2000].

[19] A rooting depth of 50 cm for the soil profile with a parallel soil columns concept was used to characterize the AMSR-E soil moisture footprints, keeping in view the scope and objective of this study. For the SWAP model simulations, the 50-cm-thick soil profile at each remote sensing footprint was discretized into 50 nodes, with finer discretization near the soil layer interfaces and at the land-atmosphere boundary. Finer discretizations near the top boundary and at layer interfaces were used to handle the steep pressure gradients for the numerical simulations. A time-dependent flux-type top boundary condition was applied for each parallel soil column matching the AMSR-E footprint. A unit vertical hydraulic gradient (free drainage) condition was used at the bottom boundary of the soil profile because of shallow root zone (50 cm). Given the relatively coarse horizontal scale with shallow root zone, the parallel soil column model ignores the lateral water fluxes across the adjacent soil columns and only predicts infiltration, evapotranspiration, and deep percolation following the parallel noninteracting stream-tubes concept of distributed vadose zone hydrology.

[20] Within the modeling domain, stochasticity was considered for soil hydraulic parameters as described in

section 2.1. However, other sources of stochasticity (e.g., uncertainty in forcing data) also exist but are not considered for the study. So, a quasi-stochastic approach was implemented in this study, where soil parameters were stochastic and forcings were deterministic (i.e., average values). Such an approach was adopted because making a model fully stochastic increases the modeling dimensions by manyfold and is extremely difficult to manage. For this study it is also assumed that the uncertainties and modeling errors introduced in simulated soil moisture values that propagate in time for such quasi-stochastic setup were reduced by precipitation events.

2.3. Site Description

[21] To study the MCMC based parameter upscaling and SVAT modeling for evaluating soil moisture dynamics in large space-borne AMSR-E footprints, diverse hydroclimatic regions within the United States were selected. As illustrated in Figure 2, large regional areas in Arizona (semiarid), Oklahoma (grassland/pastures), and Iowa (agricultural) were selected for the study. All of these regions have been included in previous hydrologic field campaigns (e.g., Southern Great Plains 1997 (SGP97), 1999 (SGP99), Soil Moisture Experiment 2002 (SMEX02), 2003 (SMEX03), 2004 (SMEX04), and 2005 (SMEX05)) whose objectives included calibration and validation of remotely sensed geophysical variables, especially soil moisture. The selected Arizona region comprises 42 AMSR-E footprints covering nearly 26,250 km². The landscape consists of perennial shrub cover with low LAI (<1 m²/m²), well-drained gravelly sandy loam soil, and moderately rocky and hilly terrains. The Oklahoma regional site encompasses 45 AMSR-E footprints covering nearly 28,125 km². Grassland and pasture with rolling topography dominates the landscape, with LAI averaging between 3 and 4 m²/m² and attaining peak value between late spring and summer.

Loamy sand, sandy loam, loam, and silty loam are the predominant surface soil textures in the Oklahoma region. The Iowa region, with 35 AMSR-E footprints spanning 21,825 km², has mainly a row crop agricultural landscape (nearly 60% corn and 40% soybeans in 2002). This site is considered as the pothole region of Iowa because of its undulating terrain. The soil on the surface is mainly silty clay loam with a large percentage of organic matter. During the peak crop growing condition the LAI for this region reaches a high of 4–6 m²/m².

2.4. Data

2.4.1. AMSR-E Soil Moisture Product

[22] For this study we used 2 years (2004–2005) of AMSR-E Level-2B data extracted for the three regions (Arizona, Oklahoma, Iowa), that was obtained from the NASA Jet Propulsion Laboratory. This Level-2B land surface product includes daily measurements of surface soil moisture, vegetation water content interpretive information, and quality control variables. The data values correspond to a ~60 km mean spatial resolution for AMSR-E at 10.7 GHz. Note that there is a difference between the spatial resolution of the AMSR-E instrument and its spatial sampling. The AMSR-E instrument samples in time every 2.6 ms at the lower frequencies [Njoku *et al.*, 2003]. During this time, the antenna motion along scan and the spacecraft motion along track result in successive samples being spaced approximately 10 km apart when projected at the Earth's surface. At each sample point, since the antenna beam has a certain width, the instrument receives radiation from a fairly broad region at the surface, i.e., the footprint or instantaneous field of view (IFOV). The footprint is normally defined by the 3-dB width of the beam, which when projected on the Earth's surface covers an elliptical region of dimension 74 km × 44 km (at 10.7 GHz), or approximately 60 km (average). So at each sample point, the measurement can be considered representative of radiation received from a footprint of dimension 60 km, even though it is sampled every 10 km. This means that the region observed in successive samples has considerable overlap, i.e., there is significant over-sampling, and each measurement is not strictly an independent observation of a fully separate region of terrain. These 10-km samples are defined in a reference coordinate system determined by the conical scan of the antenna and the forward motion of the spacecraft, forming a helical scan trace at the Earth surface. Hence the samples are often more conveniently remapped onto Earth-fixed coordinate grids (EASE-grid in our case) which could have any desired spacing (e.g., 25 km). The more reliable nighttime AMSR-E data [Njoku *et al.*, 2003] were used, as soil moisture and temperature profiles remain more uniform, and soil-vegetation temperature differences are smaller during the night than the early afternoon. In other words the soil moisture retrieval algorithm is expected to have less error and be more representative of deeper soil layers using the nighttime data.

2.4.2. TRMM and Other GPCP Calibrated Data for Precipitation

[23] Precipitation is arguably the most critical input for accurate soil moisture modeling. We used Tropical Rainfall Measuring Mission (TRMM) and other Global Precipitation Climatology Project (GPCP) calibration rainfall product 3B-42 (available at <http://disc.sci.gsfc.nasa.gov/data/datapool/>

http://disc.sci.gsfc.nasa.gov/data/datapool/TRMM/01_Data_Products/02Gridded/index.html). The combined instrument rain calibration algorithm (3B-42) uses an optimal combination of products from other satellites to adjust instantaneous rain (IR) estimates from geostationary IR observations. The rainfall data product used in this study has a spatial resolution of 0.25° × 0.25° grid for every 3 h.

2.4.3. MODIS Data for LAI

[24] Eight-day composite LAI data (from the MODIS instrument on the Terra satellite) (<http://nsidc.org/~imswww/pub/imswelcome/index.html>) with 1-km spatial resolution were used for the study. For soil moisture modeling, the MODIS data were averaged up from 1 km to ~60 km resolution to match the AMSR-E mean spatial resolution.

2.4.4. NCEP/NCAR Reanalysis Data for Atmospheric Forcings

[25] The atmospheric forcing data such as relative humidity, air temperature, etc., required for soil moisture modeling was acquired from the 40-year reanalyses products of NCEP (<http://www.cdc.noaa.gov/cdc/data.ncep.reanalysis.surfaceflux.html>). The NCEP/NCAR 40-year reanalysis uses a state-of-the-art global data assimilation system and a complete available database [Kalnay *et al.*, 1996].

2.4.5. SSURGO Data for Soil Texture

[26] Soil texture information (fraction of sand, silt, and clay) was required for generating the ensemble of upscaled soil hydraulic parameters. The data were obtained from the Soil Survey Geographic (SSURGO) database (http://www.ncgc.nrcs.usda.gov/products/data_sets/ssurgo/). SSURGO is the most detailed level of soil mapping done by the Natural Resources Conservation Service (NRCS). Mapping scales generally range from 1:12,000 to 1:63,360.

3. Results and Discussion

3.1. Upscaled Soil Hydraulic Parameters

[27] The approach described above was applied in the Arizona, Oklahoma, and Iowa regions, each encompassing several AMSR-E footprints. The SVAT model was run within the MCMC framework for 1 complete year (2004). The soil moisture evolutions from first 2 months (January and February 2004) were not used in evaluating the proposal probability distribution of soil hydraulic parameters during the MCMC runs (as mentioned in section 2.1, ii.2). This was necessary to eliminate the effects of initial conditions imposed across the profile of soil layers. Soil moisture states at the land surface were selected for 30 d in 2004 coinciding with the AMSR-E footprints to evaluate the proposal probability in MCMC sampling. A key issue in successful implementation of MCMC sampling is the number of runs (steps) until the chain approaches stationarity (length of the burn-in period). A poor choice of starting values and/or proposal probability distribution of soil hydraulic parameters can greatly influence the required burn-in time. The use of the SSURGO database for soil texture information, and corresponding parameter distributions from the UNSODA database, eliminated the possibility of choosing poor starting values from proposed parameter distributions. For this study, the MCMC chain was run 50,000 times, and the first 5000 burn-ins were discarded.

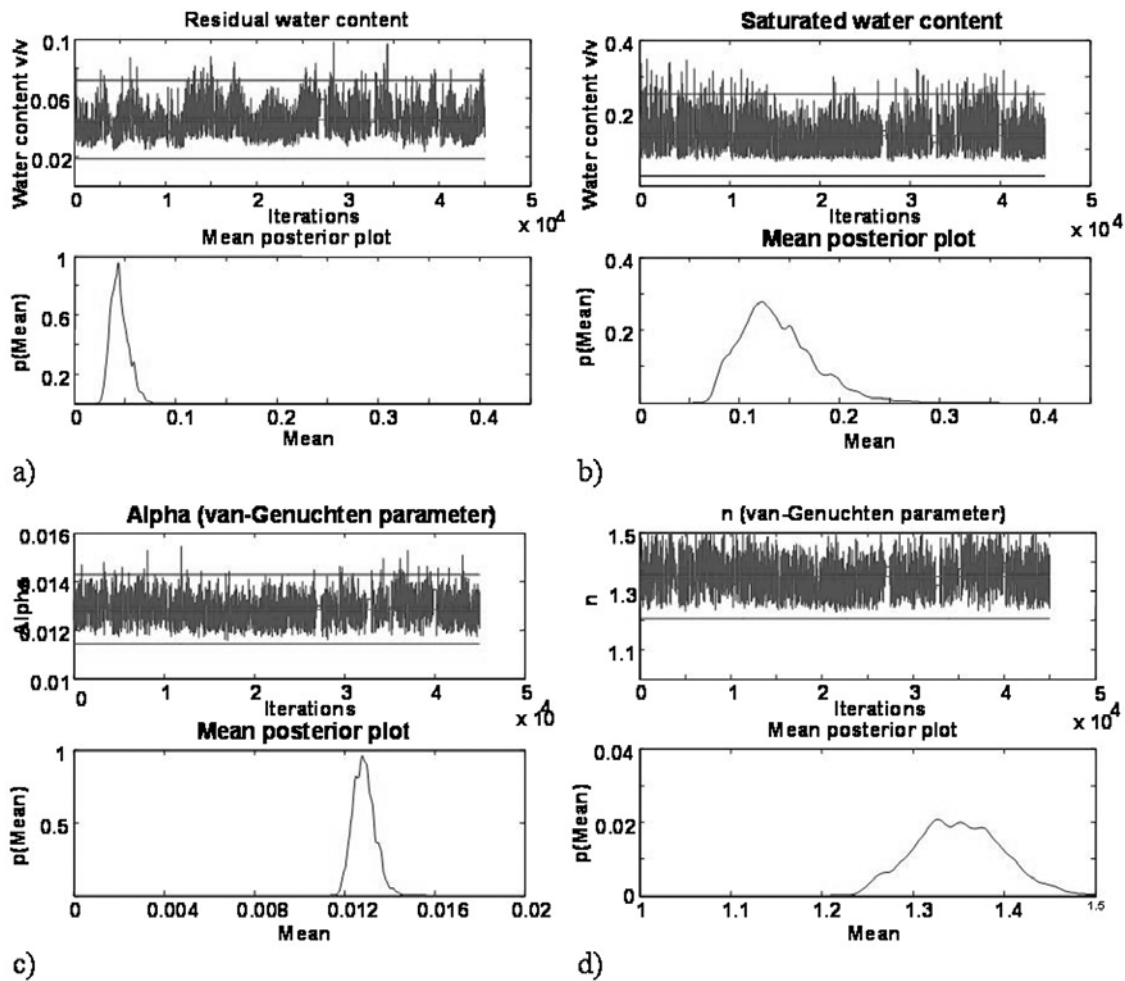


Figure 3. Posterior density plots for upscaled van Genuchten parameters, for a particular footprint in the Arizona regional site.

An acceptance ratio of nearly 7–10% was realized during MCMC for all the AMSR-E footprints used in the study. For illustration, the mixing of chain (evolution of soil hydraulic parameters from MCMC) for upscaled parameters (θ_{res}^β , θ_{sat}^β , α^β , n^β) selected randomly at the AMSR-E footprint scale from the Arizona, Iowa, and Oklahoma regions are shown in Figures 3a–3d, 4a–4d, and 5a–5d, respectively. Visual examination of these plots indicates reasonably good mixing i.e., sampling from all valid probability space. However, the length is too large (45,000) to rely upon visual inspection. Hence we considered convergence diagnostics based on the Geweke test [Geweke, 1992]. The Geweke test splits the MCMC chain (after removing the burn-in period) into two parts. The first part comprises the beginning 10% of the chain, and the second part is the last 50% of the chain. If the chain is at stationarity, the mean of the two parts should be equal, and the resulting test statistic is often referred to as the Geweke z-score. A value of greater than 2 for the Geweke z-score indicates that the mean of the series is still drifting, and a longer burn-in period is required. During the MCMC process for parameter upscaling, convergence diagnostics of the Geweke test detected no z-score greater than 2. A z-score less than 2 is also indicative of time invariant soil parameters within the footprint. The accepted proposals were extracted from the MCMC chain and subjected to a

thinning process to reduce autocorrelation. From the thinning process an ensemble of upscaled soil hydraulic parameters were prepared for the SVAT model simulation.

[28] The upscaled soil hydraulic parameters of the study regions (section 2.2) from the MCMC process were greatly influenced by the initial proposal distributions of the parameters. For the Arizona region, the initial parameter space was defined based on the dominant soil type, i.e., mostly sandy loam with a high percentage of gravel. On the other hand, the Iowa region topsoil is mostly silty clay and loam, and in the Oklahoma region the topsoil layer is dominated by fine sandy loam, clay and occasional loam. Although, the initial distributions of the parameters were predefined, the Markov random process drew samples from a very relaxed search space provided for all the parameters. The signature of soil types for the three regions is clearly visible in the PDFs of the hydraulic parameters, shown in Figures 3a–3d, 4a–4d, and 5a–5d. As expected, the mean upscaled residual water content θ_{res}^β in Arizona was the lowest of the three regions. As illustrated in Figure 5a, the effect of clay and fine sandy loam soil in Oklahoma region is also evident with highest mean θ_{res}^β . The observed variance of upscaled residual water content θ_{res}^β was quite low and very similar for all the three regions. Similarly, increasing trend for saturated water content θ_{sat}^β was also

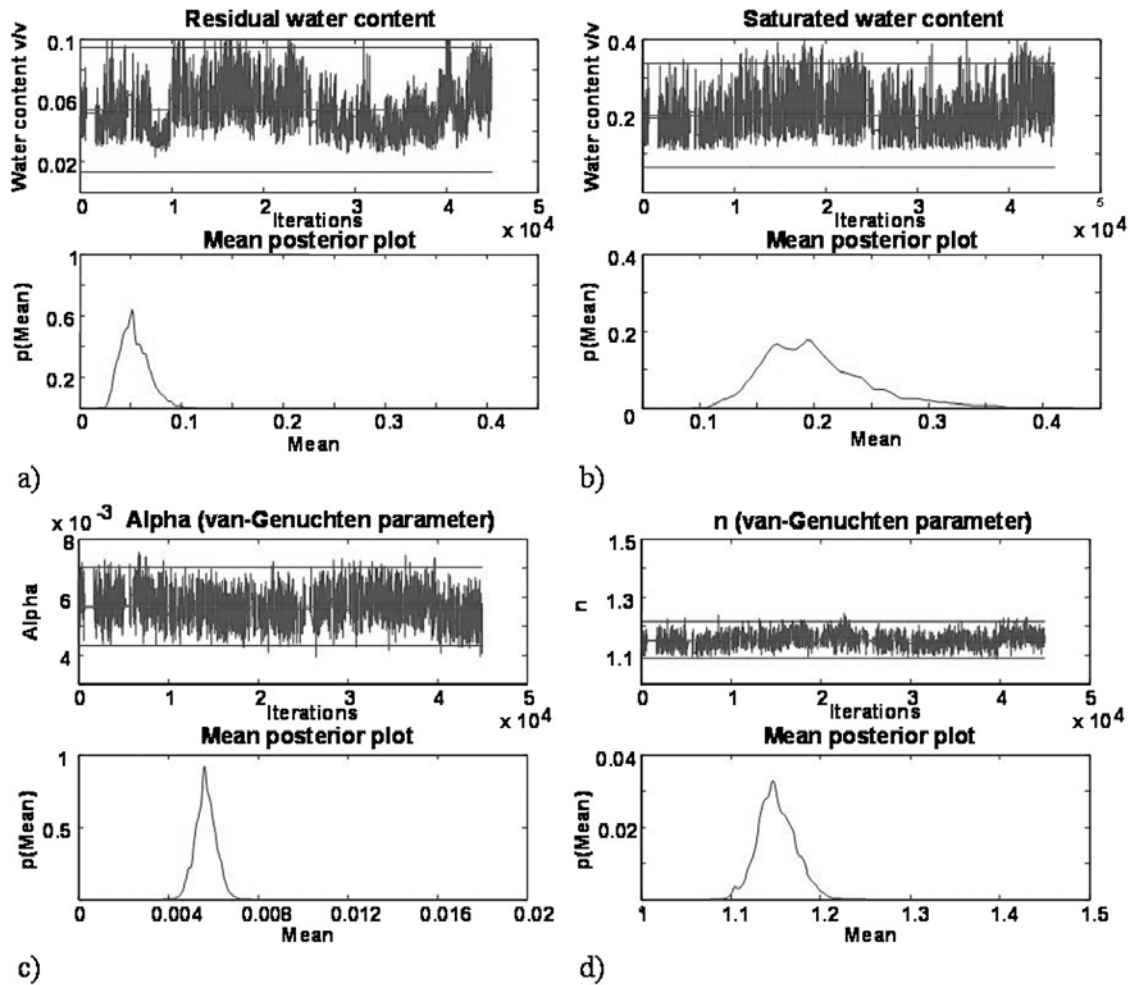


Figure 4. Posterior density plots for upscaled van Genuchten parameters, for a particular footprint in the Iowa regional site.

observed from sand and gravel dominated soil in Arizona to clayey and fine sandy loam soils in Oklahoma, revealing the influence of the parameter space in the MCMC algorithm. The variance of θ_{sat}^β encountered was also larger for the Oklahoma region than for the other two regions, determined primarily by the soil texture present in the regions. The van Genuchten parameters (α^β , n^β) show a trend with the highest mean observed for the Arizona region and lowest for the Oklahoma region, consistent with the dominant soil texture for each region. The characteristics of the hydraulic parameters shown in Figures 3a–3d, 4a–4d, and 5a–5d is typical of these particular regions. Of all the van Genuchten parameters, the saturated hydraulic conductivity (K_{sat}^β) was the most variable and uncertain parameter obtained from the upscaling algorithm. Figure 6 illustrates the probability distribution of K_{sat}^β for a typical footprint from the Arizona region. Unlike other parameters, K_{sat}^β shows a multimodal distribution in space. Similar multimodal PDFs were also observed for the Iowa and Oklahoma regional sites. Studies have shown that saturated hydraulic conductivity is a highly uncertain parameter that varies widely at the field scale [Mohanty *et al.*, 1994a]. The wide range of K_{sat}^β in a footprint scale is a fair estimation keeping in view the size of the spatial domain of this study. The MCMC-based upscaling of soil hydraulic parameters results in an effective ensemble of

parameter sets that is specific to regional hydroclimatic conditions, vegetation, and soil type. Influence of topography on upscaling of soil hydraulic parameters was not considered in this framework. However, with the parallel stream-tube concept and the large horizontal spatial extent (60 km \times 60 km) compared with the vertical range of topographic variations, the effect of topography on soil hydraulic parameters is greatly diminished.

[29] Figures 7a–7c illustrate the posterior distribution of the upscaling parameter β for the three study regions. It also exhibits typical characteristic behavior as influenced by the parameter search space of the field-scale soil hydraulic parameters. For flat homogenous bare soil the value of β is 1 and the parameter values are independent of spatial scale. With heterogeneity the value of β remains no longer equal to unity and in fact can be larger or smaller than 1. In this study the upscaling parameter β is smaller than 1 due to heterogeneity introduced by soil types, vegetation, and atmospheric forcings with increasing spatial scale. Essentially, all the nonlinearity encountered in the physical processes with increasing spatial scale is lumped in the upscaling factor β . As shown in Figure 7, the MCMC converges to a stationary distribution of β with a mean of nearly 0.8, 0.85, and 0.9 for the Arizona, Iowa, and Oklahoma regions, respectively. Mean value of β may

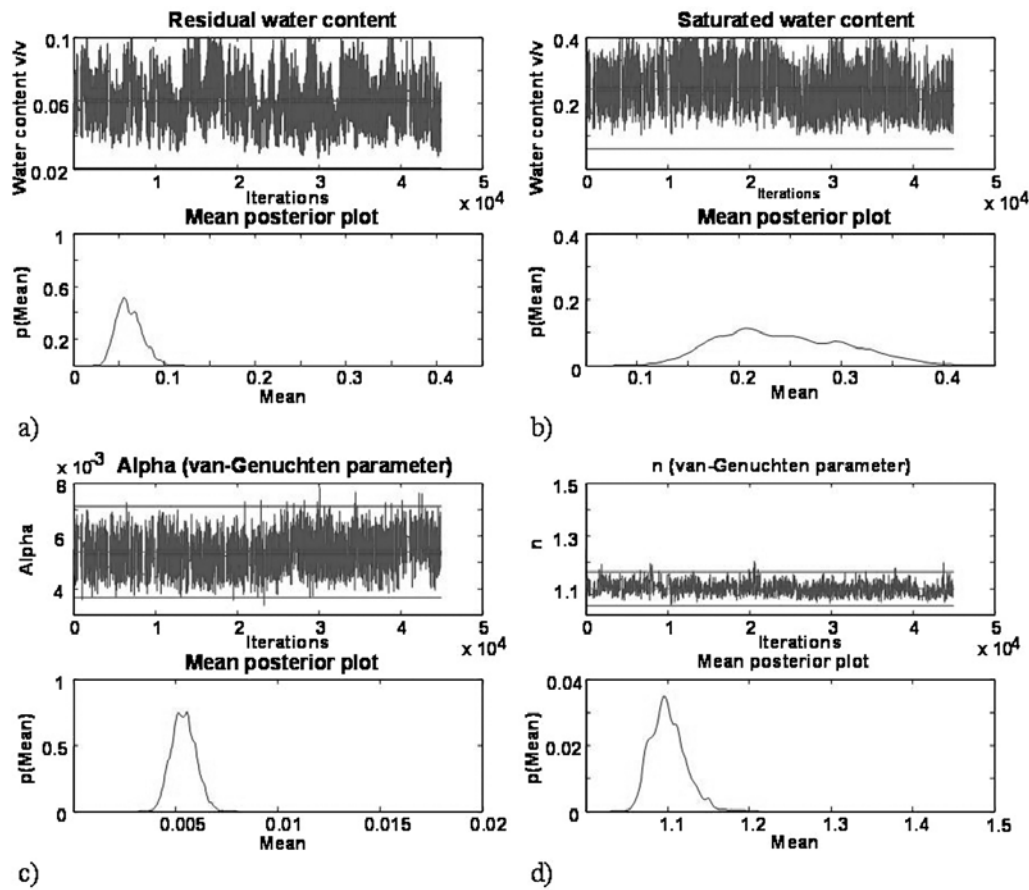


Figure 5. Posterior density plots for upscaled van Genuchten parameters, for a particular footprint in the Oklahoma regional site.

depend upon the individual AMSR-E footprint, as every footprint is unique due to complex combination of topography, vegetation, soil, and other geophysical processes. Further investigation is required to study the influence of individual as well as different combinations of geophysical parameters (soil type, topography, vegetation, and atmospheric forcings) on the behavior of β with increasing spatial scale.

3.2. Comparison of Modeled and Remotely Sensed Soil Moisture

3.2.1. Arizona Regional Site

[30] The Arizona regional site is ideal for satellite-based passive microwave remote sensing of soil moisture because of sparse vegetation ($LAI < 1 \text{ m}^2/\text{m}^2$). Studies [Njoku and Li, 1999; Paloscia et al., 1993] have demonstrated that at the AMSR-E frequency of 10.7 GHz used for soil moisture sensing, the sensitivity of brightness temperature (T_b) to variations in soil moisture strongly decreases when the soil is covered with well-developed vegetation. Also, the predominant sandy texture soil with sparse vegetation of this region is suitable for microwave remote sensing. Therefore we used this regional site as a test bed to evaluate the MCMC algorithm developed for upscaling of soil hydraulic parameters. One hundred ensemble members (each member representing one set of upscaled van Genuchten parameters) were selected from the thinning operation of the MCMC chain (posterior distribution). Modeled soil moistures from

the top 1 cm depth of the soil profile from all 42 AMSR-E footprints in the region were compared with the AMSR-E measurements. Three out of 42 footprints in the region were randomly selected to display the results of SVAT modeling of the 100 ensemble members (Figures 8a–8c) at $60 \text{ km} \times 60 \text{ km}$ resolution for 2004–2005. As illustrated in Figures 8a–8c, most of the times the ensemble of SVAT

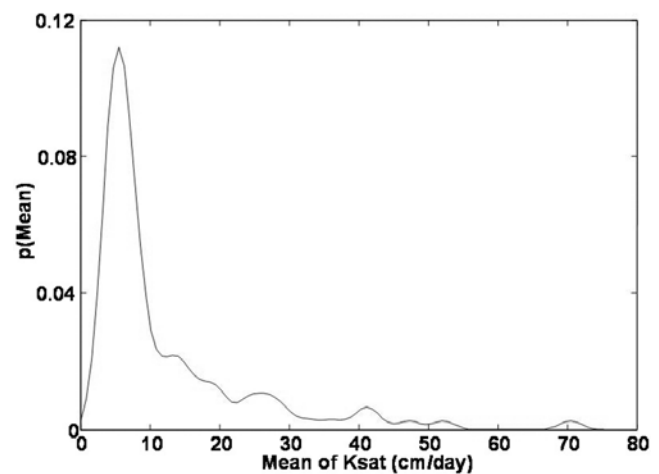


Figure 6. A typical example of probability distribution for upscaled saturated hydraulic conductivity (K_{sat}^β), from the Arizona regional site.

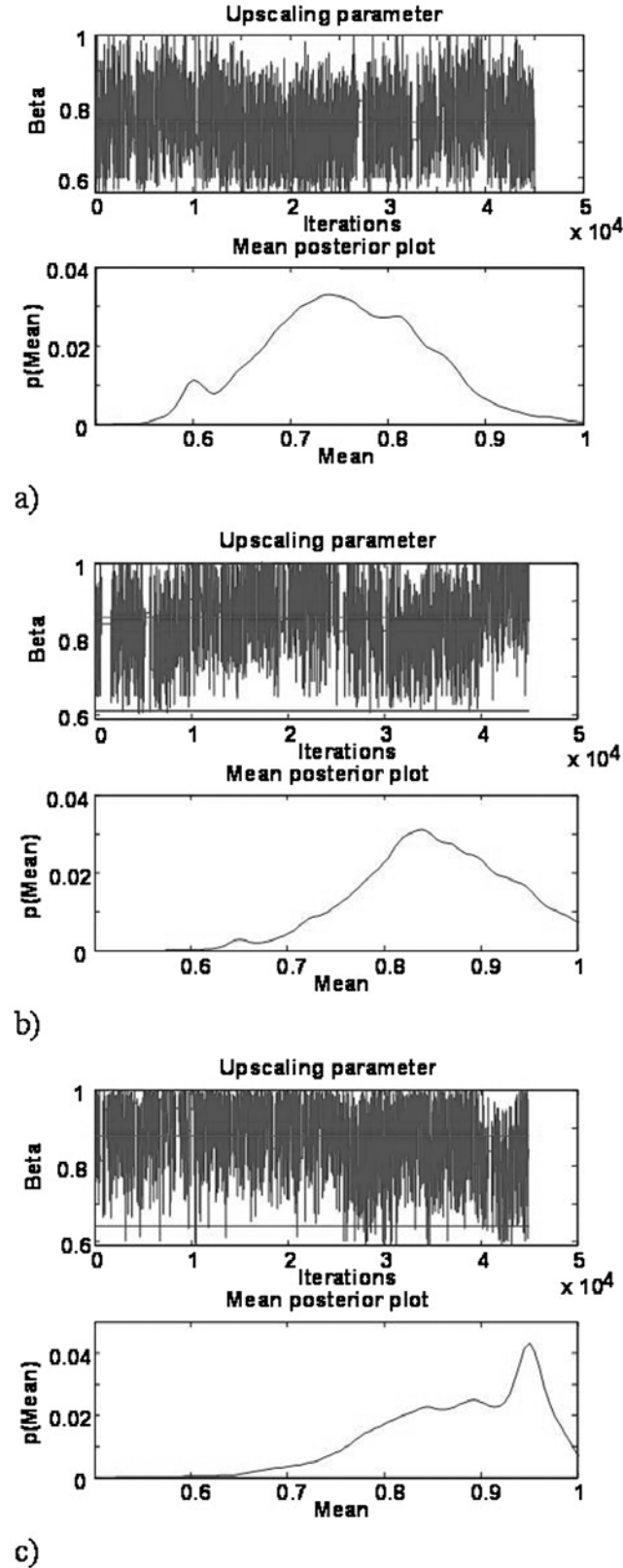


Figure 7. Posterior density plots for upscaling parameter for the (a) Arizona region, (b) Iowa region, and (c) Oklahoma region.

simulated soil moisture matches very well with the AMSR-E footprint measurements and are always within the bounds of the ensemble of SVAT simulated soil moisture. However, few discrepancies were also observed as reflected in Figure 8b. Close examination of these discrepancies reveals that the AMSR-E soil moisture data did not respond to the TRMM-based precipitation data. The reason may be the precipitation event occurring after the overpass time of the Aqua satellite (descending, 1:00 A.M.) and vice versa. The topsoil, which mostly contributes to the microwave emission, has high rock and gravel fraction with sandy texture. This influences the soil hydraulic characteristics, making them highly nonlinear with very high saturated hydraulic conductivity, which drains the soil rapidly and the signature of the precipitation event is

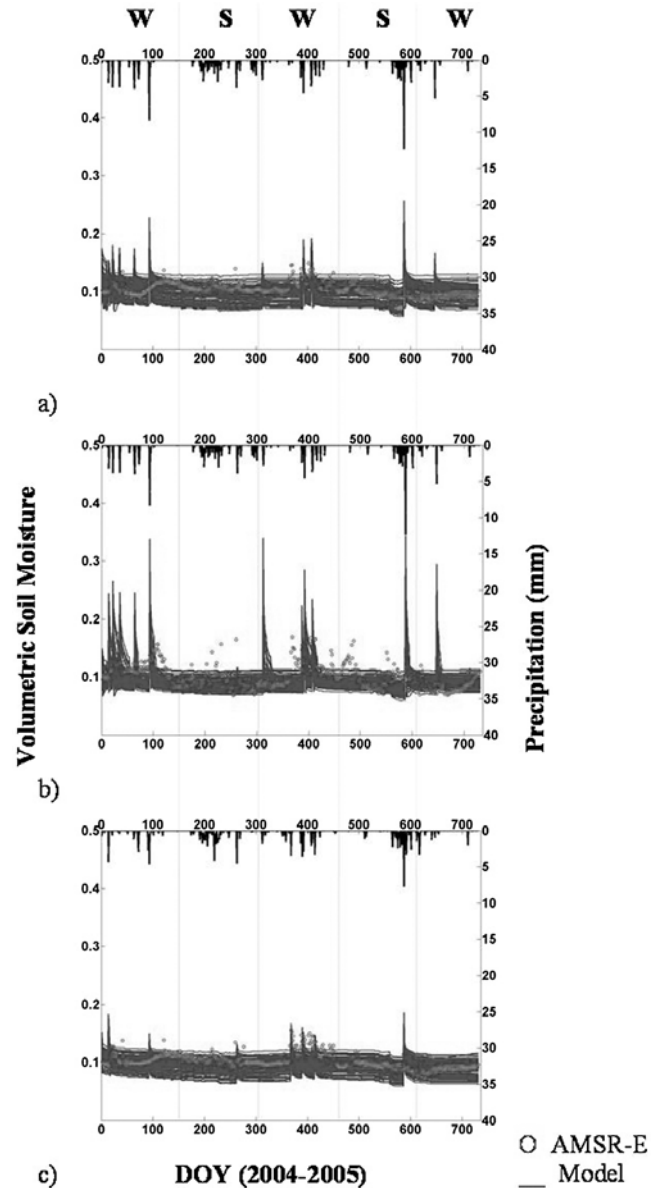


Figure 8. Comparison of randomly selected footprints of soil moisture evolution from ensemble of upscaled soil hydraulic parameters using soil-vegetation-atmosphere-transfer (SVAT) model and AMSR-E measurements for 2004–2005, from Arizona region (W, winter; S, summer).

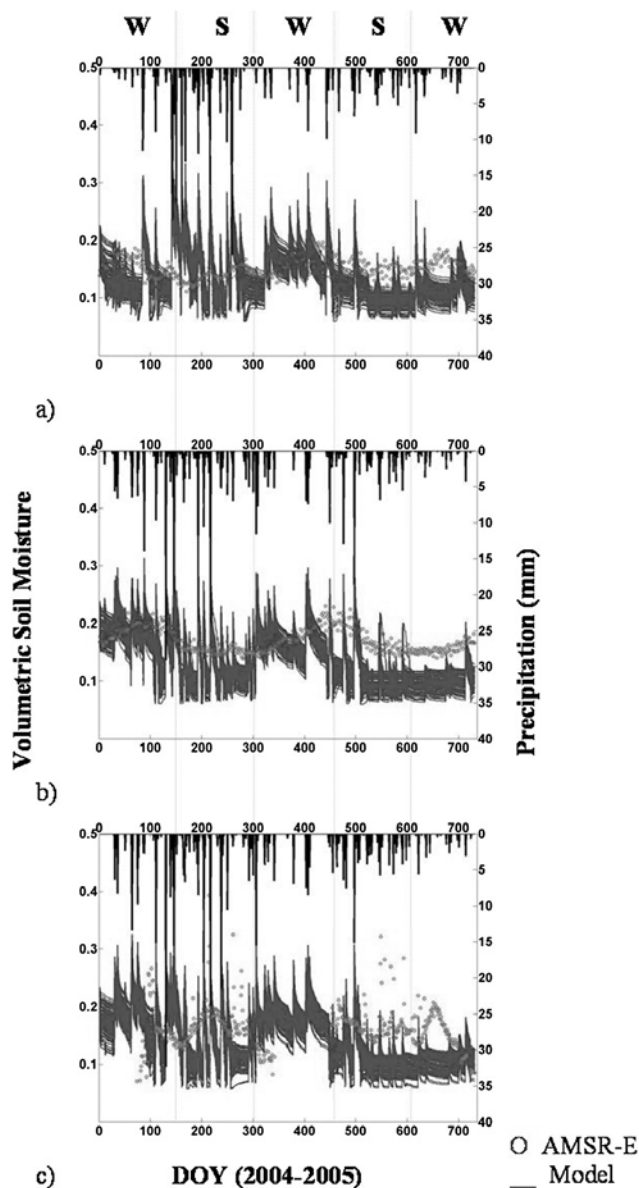


Figure 9. Comparison of randomly selected footprints of soil moisture evolution from ensemble of upscaled soil hydraulic parameters using SVAT model and AMSR-E measurements for 2004–2005, from Iowa region (W, winter; S, summer).

lost from the topsoil. During the SMEX04 field campaign, *Das et al.* [2007] also observed similar behavior in Walnut Gulch watershed situated within this Arizona regional site. A high correlation (average R of 0.91) was observed between the AMSR-E soil moisture and the mean of SVAT ensembles for all the 42 footprints during the summer seasons of 2004–2005. However, lower correlation was observed for winter periods of 2004–2005, with an average R of 0.65 (R ranging between 0.51 and 0.75). The Arizona region experiences most of the precipitation during winter by North American monsoon, which is mostly widespread and is unlike convective thunderstorms during summer. The SVAT model showed high soil moisture during such major precipitation events, whereas the AMSR-E footprints showed a weak response. This also degraded the correlation value observed during the

winter periods. Coregistration of satellite-based precipitation and soil moisture measurement may minimize such anomalies. The estimated upscaled hydraulic parameters for this region reasonably modeled the soil moisture evolution at a footprint scale. These upscaled parameters also retained the typical characteristics of the sandy soil at large scales. The good performance of SVAT model (using MCMC based upscaled parameters) with AMSR-E measurements in semi-arid Arizona region is further evaluated in agricultural landscapes with high biomass (Iowa region) and grass/pasture (Oklahoma region).

3.2.2. Iowa Regional Site

[31] The Iowa regional site is a typical example of agricultural landscape (LAI of 3–6 m^2/m^2). Using data from a soil moisture experiment (SMEX02) in June–July 2002 in this region, *Bindlish et al.* [2006] reported a satisfactory validation of the spaceborne AMSR-E soil moisture using an airborne polarimetric scanning radiometer (PSR). However, in this region, our study found contrasting results for 2004–2005. Performance of the AMSR-E soil moisture product was evaluated against the SVAT model simulated soil moisture for 35 footprints. Results from three randomly selected footprints in the region are illustrated in Figures 9a–9c. Figure 9a shows that AMSR-E did not respond to the precipitation events, especially during the summer months. This behavior was also found in many other footprints in the region (results not shown here). During summer in such agricultural regions, middle- to late-stage corn and soybean crops of high LAI (3–6 m^2/m^2) attenuate microwave emission from soil and themselves emit essentially depolarized microwave radiations [*Wang and Choudhury*, 1995]. The attenuation of microwave emission from soil introduces a masking effect observed by remote sensors and uncertainty in soil moisture process dynamics at the soil surface. Soil moisture values with very little variations or decreasing trend were found in AMSR-E measurements with the increase of LAI during the summers in the Iowa region. Contrarily, the SVAT model predictions responded with high soil moisture in the topsoil layer on the day of precipitation events. Consequently, a very low average R (0.15) was recorded between AMSR-E soil moisture product and SVAT simulated values. The region observed R values ranging from 0.11 to 0.25. A slightly higher average correlation ($R = 0.23$) was observed for the winter seasons. In a few occasions, AMSR-E soil moisture was found much higher during the winters, which may be due to wet ice. A noticeable feature in Figure 9c is high soil moisture measured by AMSR-E during the summer of 2005. This happened after small precipitation events, when the canopy interception due to high LAI reduces emissions to a large extent. At the same time, little increase in simulated soil moisture values was observed. Because of such uncertainties and overall variability, the SVAT model ensemble trajectory for the 2 years did not match well with the trend of AMSR-E measurements. A noticeable feature of this regional site is high average value and large variability in soil moisture content than the Arizona site. This finding signifies that the proposed MCMC algorithm, which retained the basic nature of the soil type after upscaling, highlights the discrepancies of SVAT modeled soil moisture evolution with the AMSR-E measurements.

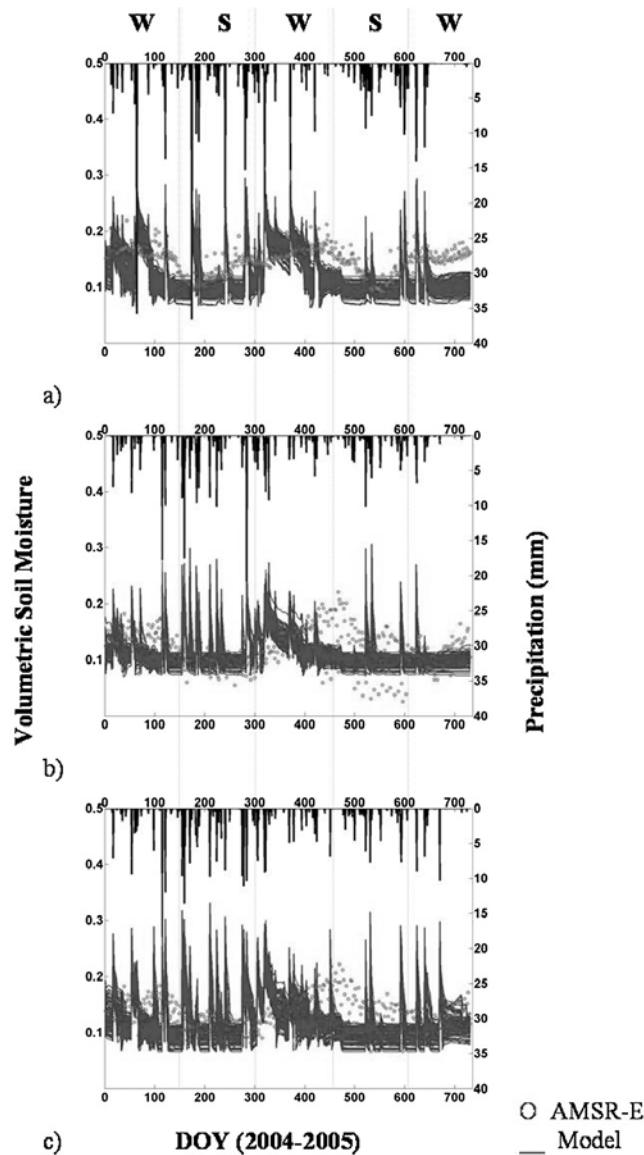


Figure 10. Comparison of randomly selected footprints of soil moisture evolution from ensemble of upscaled soil hydraulic parameters using SVAT model and AMSR-E measurements for 2004–2005, from Oklahoma region (W, winter; S, summer).

3.2.3. Oklahoma Regional Site

[32] Studies showing AMSR-E instrument validation for this region are not available to date. Other studies [Hu *et al.*, 1998, 1997; Nykanen and Foufoula-Georgiou, 2001; Oldak *et al.*, 2002; Peters-Lidard *et al.*, 2001; Rodriguez-Iturbe *et al.*, 1995] conducted in this region, using airborne remote sensing (Electronically Scanned Thinned Array Radiometer, ESTAR) soil moisture data during SGP97 field campaign reported nonstationarity and multiscaling properties with increasing spatial scale. Our MCMC-based upscaled hydraulic parameters in the SVAT model were used for 45 footprints in this region, and ensemble trajectories of soil moisture evolution for three (randomly selected) AMSR-E footprints are presented in Figures 10a–10c. The SVAT model did reasonably well as compared with the Iowa regional site. Average *R* values of 0.51 for the summers

and 0.39 for the winters in 2004–2005 were recorded for the Oklahoma region. The region observed *R* values ranging from 0.32 to 0.61. As shown in the Iowa sites, the AMSR-E footprints for Oklahoma on many occasions show no effects of major precipitation events. During the summer months, LAI of this region grows up to 3–5 m²/m², which hampers the sensitivity of AMSR-E 10.7-GHz frequency, resulting in low soil moisture values of AMSR-E footprints. It was also observed that for this regional site, the model ensemble trajectories match with the AMSR-E measurements most of the time when the LAI of this region is low.

3.3. Comparison of Ground-Based, Remotely Sensed, and Modeled Soil Moisture

[33] Extensive regional-scale field campaigns for surface soil moisture measurement (with point scale support) were conducted during the SMEX04 (in the Arizona regional site) and the SMEX05 (in the Iowa regional site). The time period of our modeling study (2004–2005) overlapped with the duration of these field campaigns. Figures 11 and 12 illustrate the comparison of surface soil moisture from SVAT model predictions, AMSR-E observations, and ground measurements (local/point scale) for the Arizona and Iowa regions, respectively. For comparison, simple average was evaluated for the all ground measurements within the specific AMSR-E grid. Note, however, the local/point scale soil moisture data (theta-probe measurements) supports a depth of 5 cm, whereas the SVAT model evolutions are from the top 1 cm and AMSR-E soil moisture data with footprint scale support are valid up to 1 cm depth. In Figure 11, the AMSR-E observations and the SVAT model predictions having footprint scale (60 km × 60 km) support maintain a steady trend without much variation, as observed in the local/point scale surface soil moisture data in the Arizona region. This is because at the footprint scale most of the local variations were homogenized, which were captured by local point scale surface soil moisture data. Also, Das *et al.* [2007] found that the change in the mean and variance of daily soil moisture probability densities at the 1 cm depth was due to the highly variable (localized) convective summer precipitation patterns across the Walnut Gulch watershed in the Arizona region. However, in the Arizona regional site the differences in mean of the surface soil moisture with SVAT model and AMSR-E soil moisture data (Figure 11) were not prominent as in the Iowa regional site (Figure 12). This was due to the prevailing dry conditions with a very conductive topsoil in the Arizona

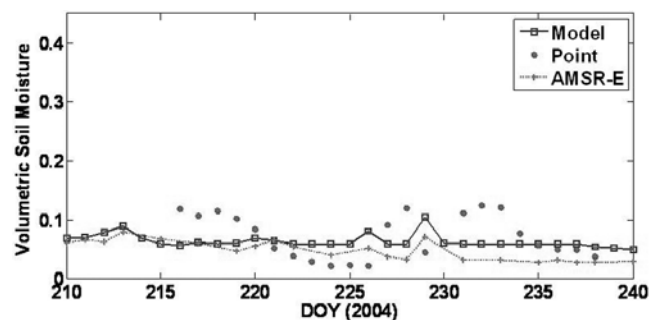


Figure 11. Comparison of field scale, SVAT model, and AMSR-E soil moisture data from Soil Moisture Experiment 2004 (SMEX04).

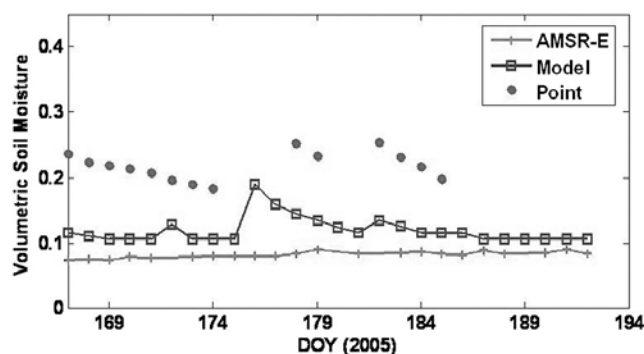


Figure 12. Comparison of field scale, SVAT model, and AMSR-E soil moisture data from Soil Moisture Experiment 2005 (SMEX05).

region. The less difference in mean soil moisture was due to no major precipitation event throughout the region during SMEX04. Therefore the wetting and subsequent dry-down phase is missing in Figure 11. Whereas, in the Iowa region, the mean of in situ surface (0–5 cm) soil moisture data is much higher than the SVAT model predictions, and the AMSR-E soil moisture data. As already discussed in section 3.2.2, high soil moisture that was measured by point-scale gravimetric sample in the clayey textured topsoil was completely masked by high LAI in the agricultural region for the AMSR-E measurements. In the Iowa region, however, the SVAT model prediction clearly responds to the precipitation events, which is not observed in the case of AMSR-E measurements because of microwave emission attenuation/manipulation by high vegetation. Another noticeable feature in Figure 12 is the difference in correlation of soil moisture of the SVAT model predictions and the point-scale measurements on wet days versus dry/dry-down days. This finding reflects the simple spatial scaling characteristics for the wet day as opposed to the multiscaling properties for the dry-down period, which corroborates the findings of *Das and Mohanty* [2008] during the SMEX02 campaign in the Iowa region. This comparison further strengthens the notion of parameter upscaling requirement and validity of using our proposed MCMC based upscaled SVAT model to record the hydrological processes within large AMSR-E footprints.

4. Conclusions

[34] It has been demonstrated that upscaling of soil hydraulic parameters from field scale to satellite footprint scale has potential for modeling soil moisture evolution at the footprint scale and for evaluating the uncertainty and limitations involved in satellite-based soil moisture data. A simple MCMC-based algorithm was developed with priors from existing field-scale soil parameters and likelihood from AMSR-E based soil moisture data to generate a posterior set of upscaled hydraulic parameters. The SVAT model used these upscaled soil hydraulic parameters in three different hydroclimatic regions to simulate the surface soil moisture for 2 years (2004–2005). A high correlation between AMSR-E soil moisture data and simulated soil moisture values was observed for the semiarid region of Arizona, attesting to the use of upscaled parameters in SVAT models at the AMSR-E footprint scale. In the

agricultural landscapes of the Iowa region, the SVAT model revealed the limitation in the AMSR-E soil moisture product under dense vegetative conditions. A very low correlation was observed in the summers of 2004–2005 for the Iowa regional site. The SVAT model did reasonably well in grass/pasturelands of Oklahoma as compared with the Iowa agricultural sites. High vegetation during summers was found to degrade the AMSR-E soil moisture detection sensitivities. One constraint encountered during this study was the precipitation inputs from TRMM, which were not coregistered with AMSR-E footprints. This led to the mismatch of soil moisture evolution from SVAT model and AMSR-E soil moisture product. Our approach, using remotely sensed data to calibrate a SVAT model to mimic the evolution of land surface state variable such as soil moisture, may be used in the future for improving the remotely sensed products through data assimilation. The technique also has the potential to derive upscaled parameters for geophysical properties.

[35] **Acknowledgments.** We acknowledge the support of NASA Goddard Space Flight Center (grant 35410), NASA (THP), and NSF (CMG/DMS) (grant 37050) for this work. We also acknowledge the support of NSIDC and NCEP/NCAR in providing data sets used for this study. This work was performed in part at the Jet Propulsion Laboratory, California Institute of Technology, under contract to the National Aeronautics and Space Administration.

References

- Bindlish, R., T. J. Jackson, A. J. Gasiewski, M. Klein, and E. G. Njoku (2006), Soil moisture mapping and AMSR-E validation using the PSR in SMEX02, *Remote Sens. Environ.*, *103*, 127–139, doi:10.1016/j.rse.2005.02.003.
- Bindlish, R., et al. (2008), Aircraft based soil moisture retrievals under mixed vegetation and topographic conditions, *Remote Sens. Environ.*, *112*(2), 375–390, doi:10.1016/j.rse.2007.06.024.
- Brooks, S. P., and G. O. Roberts (1998), Convergence assessment techniques for Markov chain Monte Carlo, *Stat. Comput.*, *8*, 319–335, doi:10.1023/A:1008820505350.
- Burke, E. J., R. J. Gurney, L. P. Simmonds, and T. J. Jackson (1997), Calibrating a soil water and energy budget model with remotely sensed data to obtain quantitative information about the soil, *Water Resour. Res.*, *33*, 1689–1697, doi:10.1029/97WR01000.
- Camillo, P. J., P. E. O'Neill, and R. J. Gurney (1986), Estimating soil hydraulic parameters using passive microwave data, *IEEE Trans. Geosci. Remote Sens.*, *GE24*(6), 930–936, doi:10.1109/TGRS.1986.289708.
- Chang, D. H., and S. Islam (2003), Effects of topography, soil properties and mean soil moisture on the spatial distribution of soil moisture: A stochastic analysis, in *Scaling Methods in Soil Physics*, edited by Y. Pachepsky et al., pp. 193–225, CRC Press, Boca Raton, Fla.
- Choudhury, B. J., T. J. Schmugge, A. Chang, and R. W. Newton (1979), Effect of surface roughness on the microwave emission from soils, *J. Geophys. Res.*, *84*, 5699–5706.
- Claussen, M. (1998), On multiple solutions of the atmosphere-vegetation system in present-day climate, *Global Change Biol.*, *4*, 4549–4560.
- Das, N. N., and B. P. Mohanty (2008), Temporal dynamics of PSR-based soil moisture across spatial scales in an agricultural landscape during SMEX02: A wavelet approach, *Remote Sens. Environ.*, *112*(2), 522–534, doi:10.1016/j.rse.2007.05.011.
- Das, N. N., B. P. Mohanty, M. H. Cosh, and T. J. Jackson (2007), Modeling and assimilation of root zone soil moisture using remote sensing observations in Walnut Gulch Watershed during SMEX04, *Remote Sens. Environ.*, *112*, 415–429.
- daSilva, A. P., A. Nadler, and B. D. Kay (2001), Factors contributing to temporal stability in spatial patterns of water content in the tillage zone, *Soil Tillage Res.*, *58*, 207–218.
- Delworth, T., and S. Manabe (1989), The influence of soil wetness on near-surface atmospheric variability, *J. Clim.*, *2*, 1447–1462, doi:10.1175/1520-0442(1989)002<1447:TIOSWO>2.0.CO;2.
- Demarty, J., C. Ottlé, I. Braud, A. Olioso, J. P. Frangi, H. V. Gupta, and L. A. Bastidas (2005), Constraining a physically based soil-vegetation-atmosphere transfer model with surface water content and thermal

- infrared brightness temperature measurements using a multiobjective approach, *Water Resour. Res.*, *41*, W01011, doi:10.1029/2004WR003695.
- Dubayah, R., E. F. Wood, and D. Lavalley (1997), Multiscaling analysis in distributed modeling and remote sensing: An application using soil moisture, in *Scale in Remote Sensing and GIS*, edited by D. A. Quattrochi and M. Goodchild, pp. 93–112, A. F. Lewis, New York.
- Foley, J. A. (1994), The sensitivity of the terrestrial biosphere to climate change: A simulation of the middle Holocene, *Global Biogeochem. Cycles*, *8*, 505–525, doi:10.1029/94GB01636.
- Gelman, A., J. B. Carlin, H. S. Stern, and D. B. Rubin (1995), *Bayesian Data Analysis*, CRC Press, Boca Raton, Fla.
- Geweke, J. (1992), *Evaluating the Accuracy of Sampling-Based Approaches to the Calculation of Posterior Moments*, pp. 169–193, Oxford Univ. press, Oxford, U.K.
- Hu, Z. L., S. Islam, and Y. Z. Cheng (1997), Statistical characterization of remotely sensed soil moisture images, *Remote Sens. Environ.*, *61*, 310–318, doi:10.1016/S0034-4257(97)89498-9.
- Hu, Z., Y. Chen, and S. Islam (1998), Multiscaling properties of soil moisture image and decomposition of large scale and small scale features using wavelet transform, *Int. J. Remote Sens.*, *19*, 2451–2467, doi:10.1080/014311698214550.
- Ines, A. V. M., and P. Droogers (2002), Inverse modeling in estimating soil hydraulic functions: A genetic algorithm approach, *Hydrol Earth Syst Sci.*, *6*, 49–65.
- Ines, A. V. M., and B. P. Mohanty (2008), Near-surface soil moisture assimilation for quantifying effective soil hydraulic properties using a genetic algorithm: 1. Conceptual modeling, *Water Resour. Res.*, doi:10.1029/2007WR005990, in press.
- Jackson, T. J., and T. J. Schmugge (1991), Vegetation effects on the microwave emission of soils, *Remote Sens. Environ.*, *36*, 203–212, doi:10.1016/0034-4257(91)90057-D.
- Jackson, T. J., R. Bindlish, A. E. Gasiewski, B. Stankov, M. Klein, E. G. Njoku, D. Bosch, T. L. Coleman, C. Laymon, and P. J. Starks (2005), Polarimetric scanning radiometer C and X band microwave observations during SMEX03, *IEEE Trans. Geosci. Remote Sens.*, *43*, 2418–2430, doi:10.1109/TGRS.2005.857625.
- Kabat, P., R. W. A. Hutjes, and R. A. Feddes (1997), The scaling characteristics of soil parameters: From plot scale heterogeneity to subgrid parameterization, *J. Hydrol.*, *190*, 363–396, doi:10.1016/S0022-1694(96)03134-4.
- Kalnay, E., et al. (1996), The NCEP/NCAR 40-year reanalysis project, *Bull. Am. Meteorol. Soc.*, *77*, 437–471, doi:10.1175/1520-0477(1996)077<0437:TNYRP>2.0.CO;2.
- Kavvas, M. L. (1999), On the coarse-graining of hydrological process with increasing scale, *J. Hydrol.*, *217*, 191–202, doi:10.1016/S0022-1694(98)00252-2.
- Leij, F. J., N. Romano, M. Palladino, M. G. Schaap, and A. Coppola (2004), Topographical attributes to predict soil hydraulic properties along a hillslope transect, *Water Resour. Res.*, *40*, W02407, doi:10.1029/2002WR001641.
- Mantoglou, A. (1992), A theoretical approach for modeling unsaturated flow in spatially variable soils: Effective flow models in finite domains and nonstationarity, *Water Resour. Res.*, *28*, 251–267, doi:10.1029/91WR02232.
- Metropolis, N., and S. Ulam (1949), The Monte Carlo method, *J. Am. Stat. Assoc.*, *44*, 335–341, doi:10.2307/2280232.
- Milly, P. C. D. (1988), Advances in modeling of water in the unsaturated zone, *Transp. Porous Media*, *3*, 491–514, doi:10.1007/BF00138613.
- Mohanty, B. P., and Z. Mousli (2000), Saturated hydraulic conductivity and soil water retention properties across a soil-slope transition, *Water Resour. Res.*, *36*, 3311–3324, doi:10.1029/2000WR900216.
- Mohanty, B. P., M. D. Ankeny, R. Horton, and R. S. Kanwar (1994a), Spatial-analysis of hydraulic conductivity measured using disc infiltrimeters, *Water Resour. Res.*, *30*, 2489–2498, doi:10.1029/94WR01052.
- Mohanty, B. P., R. S. Kanwar, and C. J. Everts (1994b), Comparison of saturated hydraulic conductivity measurement methods for a glacial-till soil, *Soil Sci. Soc. Am. J.*, *58*, 672–677.
- Monteith, J. L. (1965), Evaporation and environment, in *Proceedings of the 19th Symposium of the Society for Experimental Biology*, pp. 205–234, Cambridge University Press, New York.
- Mualem, Y. (1976), A new model for predicting the hydraulic conductivity of unsaturated porous media, *Water Resour. Res.*, *12*, 513–522, doi:10.1029/WR012i003p0513.
- Nemes, A., M. G. Schaap, F. J. Leij, and J. H. M. Wosten (2001), Description of the unsaturated soil hydraulic database UNSODA version 2.0, *J. Hydrol.*, *251*, 151–162, doi:10.1016/S0022-1694(01)00465-6.
- Njoku, E. G., and S. K. Chan (2006), Vegetation and surface roughness effects on AMSR-E land observations, *Remote Sens. Environ.*, *100*, 190–199, doi:10.1016/j.rse.2005.10.017.
- Njoku, E. G., and J. A. Kong (1977), Theory for passive microwave remote sensing of near-surface soil moisture, *J. Geophys. Res.*, *82*(20), 3108–3118, doi:10.1029/JB082i020p03108.
- Njoku, E. G., and L. Li (1999), Retrieval of land surface parameters using passive microwave measurements at 6–18 GHz, *IEEE Trans. Geosci. Remote Sens.*, *37*, 79–93, doi:10.1109/36.739125.
- Njoku, E. G., T. J. Jackson, V. Lakshmi, T. K. Chan, and S. V. Nghiem (2003), Soil moisture retrieval from AMSR-E, *IEEE Trans. Geosci. Remote Sens.*, *41*, 215–229, doi:10.1109/TGRS.2002.808243.
- Nykanen, D. K., and E. Foufoula-Georgiou (2001), Soil moisture variability and scale-dependency of nonlinear parameterizations in coupled land-atmosphere models, *Adv. Water Resour.*, *24*, 1143–1157, doi:10.1016/S0309-1708(01)00046-X.
- Oldak, A., Y. Pachepsky, T. J. Jackson, and W. J. Rawls (2002), Statistical properties of soil moisture images revisited, *J. Hydrol.*, *255*, 12–24, doi:10.1016/S0022-1694(01)00507-8.
- Pachepsky, Y., W. J. Rawls, and D. Gimenez (2001), Comparison of soil water retention at field and laboratory scales, *Soil Sci. Soc. Am. J.*, *65*, 460–462.
- Paloscia, S., P. Pampaloni, L. Chairantini, P. Coppo, G. Gagliani, and G. Luzi (1993), Multifrequency passive microwave remote sensing of soil moisture and roughness, *Int. J. Remote Sens.*, *14*, 467–483, doi:10.1080/01431169308904351.
- Peck, A. J., R. J. Luxmoore, and J. L. Stolzy (1977), Effects of spatial variability of soil hydraulic properties in water budget modeling, *Water Resour. Res.*, *13*, 348–354, doi:10.1029/WR013i002p00348.
- Peters-Lidard, C. D., F. Pan, and E. F. Wood (2001), A re-examination of modeled and measured soil moisture spatial variability and its implications for land surface modeling, *Adv. Water Resour.*, *24*, 1069–1083, doi:10.1016/S0309-1708(01)00035-5.
- Rodriguez-Iturbe, I., G. K. Vogel, R. Rigon, D. Entekhabi, F. Castelli, and A. Rinaldo (1995), On the spatial organization of soil moisture fields, *Geophys. Res. Lett.*, *106*, 2757–2760, doi:10.1029/95GL02779.
- Roth, K. H., H. J. Vogel, and R. Kasteel (1999), The scaleway: A conceptual framework for upscaling soil properties, in *Modelling of Transport Process in Soil at Various Scales in Time and Space*, edited by J. Feyen and K. Wiyono, pp. 477–490, Wageningen Pers, Wageningen, Netherlands.
- Seyfried, M. S., and B. P. Wilcox (1995), Scale and the nature of spatial variability: Field examples having implications for hydrological modeling, *Water Resour. Res.*, *31*, 173–184, doi:10.1029/94WR02025.
- Sharma, S. K., B. P. Mohanty, and J. Zhu (2006), Including topography and vegetation attributes for developing pedo transfer functions in Southern Great Plains of USA, *Soil Sci. Soc. Am. J.*, *70*, 1430–1440, doi:10.2136/sssaj2005.0087.
- Texier, D., N. d. Noblet, S. P. Harrison, A. Haxeltine, D. Jolly, S. Jousaume, F. Laarif, I. C. Prentice, and P. Tarasov (1997), Quantifying the role of biosphere-atmosphere feedbacks in climate change: Coupled model simulations for 6000 years BP and comparison with paleodata for northern Eurasia and northern Africa, *Clim. Dyn.*, *13*, 865–882, doi:10.1007/s003820050202.
- Tomer, M. D., C. A. Cambardella, D. E. James, and T. B. Moorman (2006), Surface-soil properties and water contents across two watersheds with contrasting tillage histories, *Soil Sci. Soc. Am. J.*, *70*, 620–630, doi:10.2136/sssaj2004.0355.
- Ulaby, F. T., and E. A. Wilson (1985), Microwave attenuation properties of vegetation canopies, *IEEE Trans. Geosci. Remote Sens.*, *23*, 746–753, doi:10.1109/TGRS.1985.289393.
- Ulaby, F. T., R. K. Moore, and A. K. Fung (1986), *Microwave Remote Sensing: Active and Passive*, Artech House, Norwood, Mass.
- Van Dam, J. C. (2000), *Field-Scale Water Flow and Solute Transport: SWAP Model Concepts, Parameter Estimation and Case Studies*, Wageningen Univ., Wageningen, Netherlands.
- Van Dam, J. C., J. Huygen, J. G. Wesseling, R. A. Feddes, P. Kabat, and P. E. V. Van Walsum (1997), Theory of SWAP version 2.0: Simulation of water and plant growth in the soil-water-atmosphere-plant environment, Tech. Doc. 45, Wageningen Agric. Univ. and DLO Winand Staring Cent., Wageningen, Netherlands.
- van Genuchten, M. T. (1980), A closed-form equation for predicting the hydraulic conductivity of unsaturated soils, *Soil Sci. Soc. Am. J.*, *44*, 892–898.
- Wang, J. R. (1980), The dielectric properties of soil-water mixtures at microwave frequencies, *Radio Sci.*, *15*, 977–985, doi:10.1029/RS015i005p00977.
- Wang, J. R., and B. J. Choudhury (1995), Passive microwave radiation from soil: Examples of emission models and observations, in *Passive*

- Microwave Remote Sensing of Land-Atmosphere Interactions*, edited by B. J. Choudhury et al., pp. 423–460, VSP, Utrecht, Netherlands.
- Wang, J. R., and T. J. Schmugge (1980), An empirical model for the complex dielectric permittivity of soil as a function of water content, *IEEE Trans. Geosci. Remote Sens.*, *GE-18*, 288–295, doi:10.1109/TGRS.1980.350304.
- Wesseling, J. G., and J. G. Kroes (1998), *A Global Sensitivity Analysis of the Model SWAP*, DLO Winand Staring Cent., Wageningen, Netherlands.
- Western, A. W., R. B. Grayson, and G. Blöschl (2002), Scaling of soil moisture: A hydrologic perspective, *Annu. Rev. Earth Planet. Sci.*, *30*, 149–180, doi:10.1146/annurev.earth.30.091201.140434.
- Zhang, D. X. (1999), Nonstationary stochastic analysis of the transient unsaturated flow in randomly heterogeneous media, *Water Resour. Res.*, *35*, 1127–1141, doi:10.1029/1998WR900126.
- Zhu, J., and B. P. Mohanty (2002), Spatial averaging of van Genuchten hydraulic parameters for steady-state flow in heterogeneous soils: A numerical study, *Vadose Zone J.*, *1*, 261–272.
- Zhu, J., and B. P. Mohanty (2003), Upscaling of hydraulic properties of heterogeneous soils, in *Scaling Methods in Soil Physics*, edited by Y. A. Pachepsky et al., pp. 97–118, CRC Press, Boca Raton, Fla.
-
- N. N. Das and B. P. Mohanty, Department of Biological and Agricultural Engineering, Texas A&M University, 301 C Scoates Hall, College Station, TX 77843-2117, USA. (bmohanty@tamu.edu)
- E. G. Njoku, Water and Carbon Cycles Group, Jet Propulsion Laboratory, California Institute of Technology, M/S 300-233, 4800 Oak Grove Drive, Pasadena, CA 91109, USA.